Research Square

Preprints are preliminary reports that have not undergone peer review.
They should not be considered conclusive, used to inform clinical practice,
or referenced by the media as validated information.

Field and Experimental Investigations of the Effect of Hyporheic Exchange on Nitrogen Transport in Lakeshore Lacustrine Sedimentary Aquifers, SW China

Ronggao Qin
Kunming University of Science and Technology
Haoyi Li
Kunming University of Science and Technology
Wan Xu
Kunming University of Science and Technology
Ciming Kong
Qujing Environmental Engineering Evaluation Center
Yiming Xie
Kunming University of Science and Technology
Guangzhu Cao
cgzhu@163.com
Kunming University of Science and Technology
Ruoyu Mao
Kunming University of Science and Technology
Yi Qiang
Kunming University of Science and Technology
Yanfeng Lu
Kunming University of Science and Technology

Research Article

Keywords: Hyporheic exchange, Surface water-groundwater exchange, Lacustrine sedimentary aquifer, Nitrogen transport, Erhai Lake

Posted Date: March 4th, 2026

DOI: https://doi.org/10.21203/rs.3.rs-8105170/v1

License: This work is licensed under a Creative Commons Attribution 4.0 International License.
Read Full License

Additional Declarations: No competing interests reported.

Abstract

In recent years, many plateau lakes have faced a high risk of eutrophication. Sewage interception engineering measures have been implemented around these lakes to reduce the discharge of nitrogen and phosphorus. However, these measures often overlook the exchange between surface water, the hyporheic zone, and groundwater, as well as the mechanisms of nutrient transport and transformation in the engineering area near the lakes. This study investigates the interaction mechanisms of surface water, hyporheic zones, and groundwater and their impact on nitrogen transport following the implementation of sewage interception engineering on the west bank of Erhai Lake in Yunnan Province, China, by combining field investigations and laboratory tracer experiments. Field monitoring results show that hyporheic flux is closely related to seasonal variations in river levels. Flow and tracer transport tests reveal significant differences between the flow patterns in the wet and dry seasons in the hyporheic zone near the lake. Processes such as cation adsorption, denitrification, nitrification, and dissimilatory reduction during the exchange of surface water, hyporheic flow, and groundwater mean that nitrification dominates nitrogen transformation in shallow soil. Denitrification and dissimilatory reduction in deep soil significantly affect nitrogen conversion. The groundwater nitrate content increases with the duration of pond or drain infiltration near the upstream of the lake. This investigation provides insights into flow and nitrogen transport within surface water-groundwater systems and offers a valuable reference for assessing the risk of lake eutrophication in similar lakeshore lacustrine sedimentary aquifers.

1 Introduction

The water scarcity will influenced by the future nitrogen pollution worldwide (Wang et al., 2024a). The dynamics of groundwater-surface water interactions and their effect on the transport and fate of nitrogen have been a subject of widespread concern (Guo et al., 2023; Hare et al., 2021; Lewandowski et al., 2024; Lu and Yang, 2024; Partington et al., 2023; Valett and Reinhold, 2022; Zuo et al., 2023). Exchanges between surface water and groundwater occur not only on a regional scale (Bouchez et al., 2021; Xu et al., 2021) but also on a continental scale (Hare et al., 2021). Basilio Hazas et al. (2023) evaluated the solute plume geometry, dilution, and reactive mixing transport in porous media at the surface water-groundwater interface under laboratory scale through experiments and simulations. Marti et al. (2023) investigated groundwater flow and surface water-groundwater interaction in mountain systems by combining multiscale geological mapping, geophysics, and hydrological data. Hingst et al. (2023) found that surface water-groundwater connections lead to the salinization of inland aquifers.

The interaction between surface water and groundwater, along with anthropogenic activities resulting in nitrate contamination, has also attracted extensive attention. This includes the effect of urbanization on regional-scale surface water-groundwater interaction and nitrate transport (Yifru et al., 2022), the influence of preferential flow and tides on pore water flow and marine nitrogen transport reactions in coastal aquifers (Gao et al., 2024a), fully integrated numerical simulations of surface water-groundwater interactions (Jafari et al., 2021), and nitrate transport in coupled surface-subsurface hydrologic systems

(Wei et al., 2019; Zhang et al., 2024a), and nitrate transport in stream water-groundwater interaction systems (Xia et al., 2024). The surface and groundwater nitrate contamination in the binate cropland watershed have also been studied (Assa et al., 2024).

The hyporheic zone is a critical interface for groundwater and surface water interactions in streams and rivers. Near-surface aquifers that interact with surface water are referred to as 'hyporheic zones' (Gooseff, 2010). The exchange of mass and energy within hyporheic zones is crucial for understanding these interactions. Over the past few decades, the hyporheic zone has attracted widespread attention. Studies have included hyporheic flux monitoring by temperature sensing (Briggs et al., 2012; Gordon et al., 2012), the impact of heterogeneity and anisotropy on hyporheic exchange (Chen and Zeng, 2015; Earon et al., 2020; Laube et al., 2018; Nelson et al., 2019; Pryshlak et al., 2015; Suning and May, 2018; Zhou et al., 2014), and the effects of low-permeability layers on the spatial patterns of hyporheic exchange and groundwater upwelling (Gomez-Velez et al., 2014). Additionally, the influence of stream flow, ambient groundwater, and sediment anisotropy on hyporheic zone characteristics in alternate bars (Monofy and Boano, 2021), as well as hyporheic exchange influenced by cobbles on sandy beds (Lee et al., 2022) and by fractures in sedimentary rock riverbeds (Chow et al., 2021), have been explored. Human engineering activities' impact on hyporheic exchange has also garnered attention, including investigations through laboratory experiments with spur dikes (Zhuang et al., 2023) and numerical modeling (Ren et al., 2023), and the effect of subsurface structures and steps on hyporheic exchange (Tajari et al., 2023).

On the other hand, solute and contaminant transport within the hyporheic zone is crucial for water environmental protection. Zhu et al. (Zhu et al., 2023) explored the competition between heterotrophic denitrification and DNRA pathways in the hyporheic zone and its impact on nitrate fate. S Gao et al. (2024b) used numerical models to study the combined effects of aquifer heterogeneity and subsurface dams on nitrate contamination in coastal aquifers. Marzadri et al. (2024) examined the effects of hydraulic conductivity stratification on hyporheic flows and solute residence time distribution. The nutrient pollution and cycle within the hyporheic zone are vital for managing surface water and groundwater contamination. The mixing effects on nitrogen and oxygen concentrations and their relationship to mean residence time in a hyporheic zone of a riffle-pool sequence were studied by Naranjo et al. (2015). The effects of turbulence-driven hyporheic flow and denitrification on nitrogen removal (Li et al., 2017), denitrification in the banks of fluctuating rivers (Shuai et al., 2017), and denitrification in riparian zones (Lutz et al., 2020) have also been of interest, as well as hyporheic denitrification caused by a peak flow event (Lotts and Hester, 2022).

More recently, studies have focused on the transport of phosphorus in the hyporheic zone (Jin et al., 2022), hyporheic exchange and nitrogen cycle processes under the dual effects of flooding and heterogeneous streambed (Lin et al., 2023), the effect of particulate organic carbon deposition on nitrate reduction in the hyporheic zone (Ping et al., 2023), the coupling of nitrogen and sulfur cycling in the hyporheic zone of effluent-dominated rivers (Wang et al., 2024b), and the influence of point bars on nitrogen transport and reaction in riparian zones (Song et al., 2024). Recent studies by Zhang et al.

(2024b) have examined the interaction between surface water and groundwater, along with solute transport at the sediment-water interface in the Poyang Lake basin. They employed indoor experiments and simulations based on real topography to investigate how the separation distance and elevation differences between two seasonal lakes contribute to increased solute transport from the nearer lake to the main lake. This process leads to a higher flux of pore water into the overlying water and promotes downward solute transport in the lakebed, similar to the sewage interception engineering pond around the west side of Erhai Lake in this study. A multi-tracer approach was used by Xia et al. (2024) to identify the response of nitrate dynamics to surface water-groundwater (SW-GW) interaction in the Fen River Basin. The concentrations of NO_3^- in stream water and groundwater varied significantly across different locations and times. Sewage and manure (28%–73%), fertilizer (14%–36%), and soil organic nitrogen (12%–28%) were identified as the primary NO_3^- sources in these water bodies. Additionally, in gaining streams, groundwater dilutes the nitrate content of stream water, which increases with the infiltration time of stream water. However, nitrogen concentrations in groundwater discharging into streams were highly heterogeneous, varying twentyfold along the mainstem (Moore et al., 2023).

Topography and geomorphology factors of the plateau, as shown in Fig. 1, control variability. The main recharge sources for surface water in typical plateau lakes include surface water runoff, lateral groundwater recharge, and base flow. With the rapid development of agriculture and tourism around lakes, eutrophication is intensifying, as noted by (Cui et al., 2023; Lin et al., 2021; Ni et al., 2016; Wang et al., 2023). Over the past two decades, numerous studies have focused on the eutrophication of Erhai Lake, China, due to nitrogen release at the water-sediment interface (Zhang et al., 2014), organic nitrogen from Lake Erhai sediment (Li et al., 2016; Ni et al., 2016), dissolved organic phosphorus inputs (Ji et al., 2017), and sustainable development and environmental restoration (Lin et al., 2020), along with eutrophication assessment and management (Lin et al., 2021). Eutrophication in Erhai Lake has worsened since around 2000. Over the past decade, the implementation of the lake-wide pollution control projects around Erhai Lake has been effectively reduced the discharge of rural domestic sewage and agricultural non-point source pollution wastewater into the lake. As shown in Fig. 2, streams and drainage from the Dali ancient city flowing to Erhai Lake are intercepted by sewage interception engineering near the lakeshore. The collected sewage flows from northwest to southeast along several artificial ponds and wetlands and is finally discharged into Erhai Lake by the Baihe stream. However, Fig. 2 also shows that the growth of phytoplankton in coastal waters outside the sewage interception engineering zone was significantly higher than in other areas. Consequently, surface water near the shore of Erhai Lake is recharged by hyporheic exchange and base flow at the bottom of the sewage interception engineering. At the same time, nitrogen contaminants adsorbed by the original lacustrine loose sediments at the bottom of nearby villages are leached and discharged into Erhai Lake.

In this study, a hydrogeological survey of the lacustrine sedimentary layer along the lakeshore, on-site monitoring of hyporheic flux, and nitrogen contamination monitoring and analysis at different depths in rivers near the circum-lake sewage interception engineering were conducted. Finally, the potential hyporheic exchange between pond water and Erhai Lake and the mechanism of nitrogen transport

evolution after the implementation of the circum-lake sewage interception engineering were simulated using an indoor two-dimensional sandbox test.

2 Materials and Methods

2.1 Hydrology and Hydrogeology of the Study Area

Erhai Lake is situated at the eastern foot of Cangshan Mountain in the Dali Basin, western Yunnan Province (Fig. 1). The region experiences a tropical monsoon climate, characterized by small seasonal temperature variations but significant daily fluctuations. Winters are mild and summers are not excessively hot. The climate, influenced by its proximity to the Tropic of Cancer, divides into a dry season and a rainy season. The dry season typically spans six months, from November to April of the following year, contributing only 5–15% of the annual rainfall. In contrast, the rainy season lasts from May to October, bringing 85–95% of the annual rainfall with highly uneven distribution. The Eighteen Streams, located on the western side of Erhai Lake in Cangshan Mountain, is one of the lake's primary water sources. This mountainous headwater river features a short course, narrow bed, significant elevation changes, rapid flows, and large seasonal variations in water volume. The steep slopes in the upper reaches and the deep incisions of the riverbed facilitate substantial stream runoff. The total basin area is 336.9 square kilometers, and the average annual surface runoff is 233.9 million cubic meters. The river's water quality is crucial for the ecological environment of Erhai Lake.

Because of a deep fault zone beneath Erhai Lake, the geological structure of the Dali Basin is extremely complex, with a predominant from north-northwest trend. Since its formation in the Early Pleistocene, the basin has accumulated over 1,000 meters of sediments, including lacustrine deposits, fluvial content, and a proluvial fan, which together form a porous aquiferous stratum system. The Paleozoic carbonate karst aquifer mainly occupies the eastern and northern parts of the basin, while the western region is underlain by the metamorphic rocks of the Cangshan group fissure aquifer. The southern part of the basin consists of the Western Yunnan red layer, a component of the clastic rock fracture aquifer (Zhou et al., 2021).

As illustrated in Fig. 2 by Zhou et al. (2021), The Dali alluvial-proluvial fans (APFs) Basin contains 18 rivers. These rivers are distributed along the western edge of the basin across a 1 to 3 km wide area. As shown in Fig. 3 by Zhou et al.(2021), due to frequent and intermittent tectonic uplift in the Cangshan Mountains, the lithology of the APF sediments is complex. The slopes are generally steep in the upper segments and flatten in the lower segments. The aquifer primarily consists of loose, porous Quaternary sediments. The western portion of this porous aquifer, located in the Cangshan Mountains, features a prominent area of bedrock that forms a fractured aquifer (indicated by the pink area in Fig. 3 of Zhou et al. (2021)). The 18 streams in the eastern Cangshan Mountains carry surface runoff after atmospheric precipitation recharge. The water in these streams flows from west to east. The frequent and complex interactions between surface water and groundwater in the APF aquifers are due to the heterogeneity in lithofacies/hydrofacies distribution and sedimentary structure.

The bottom of the circum-lake sewage interception engineering consists of a lacustrine sedimentary layer, which lies parallel and 2 km to the west of Erhai Lake. According to hydrogeological surveys, this layer is formed from surface cultivated soil overlying a silt layer, the thickness of the surface soil varies from 0.4 to 1.2 meters.

Figure 3 indicates that farmers often dig irrigation ponds in these fields, measuring about 1 to 1.5 meters deep, 2 meters wide, and 10 meters long. These ponds seldom dry up, except during particularly dry years. Field investigations and analyses indicate that excavating around 60 centimeters in the vegetable fields west of the sewage interception engineering can expose the stable groundwater level. The groundwater level remains relatively stable, while the rise in shallow groundwater level accelerates the exchange between surface and groundwater and promotes the transport and transformation of nitrogen among soil, surface water, and groundwater.

In this study, we will monitor the hyporheic flux of the Taoxi River bed near the sewage interception engineering in the downstream area of Dali Ancient City, along with shallow groundwater nitrogen pollutants around the northernmost pond of the sewage interception engineering. By monitoring the hyporheic flux in different seasons, we aim to understand the hydrodynamic exchange mechanism between surface water and groundwater. Laboratory tests using a two-dimensional flow model will explore the potential drainage from ponds and the sewage interception engineering to the bottom of Erhai Lake, including nitrogen transport and transformation (Fig. 2). This will provide a scientific basis for subsequent control of eutrophication pollution in Erhai Lake and other similar lakes.

2.2 Monitoring and analysis method of riverbed hyporheic exchange flux in field investigation

As illustrated in Fig. 2, the circum-lake sewage interception engineering project is located between Taoxi and Baihe Stream, running nearly parallel to the western shore of Erhai Lake and perpendicular to both Taoxi and Baihe Stream, with Zhonghe Stream in the middle. To explore the interactions between surface water and groundwater near this engineering project conducted to measure the hyporheic exchange flux in the Taoxi riverbed near its intersection with the engineering project on the north side (Point A in Figure S1). The current ponds and ditches of the project extend approximately 5 km from north to south, covering the entire ancient city area (cross-section in Fig. 2). This monitoring helps estimate the potential volume of water exchanged, which is discharged to the eastern side of Erhai Lake through hyporheic exchange at the bottom of the engineering project.

The transformation and migration of heat within the hyporheic zone typically follow paths of water exchange, varying with the depth of riverbed sediments and changes in riverbed location. By employing temperature data loggers, high-density continuous monitoring of riverbed temperature profiles is achieved. This in situ temperature tracing experiment processes and analyzes riverbed temperature data using the VFLUX2 program, which is based on a one-dimensional transient vertical heat transport analytical model, to quantitatively calculate the vertical water exchange in the hyporheic zone. This research establishes a foundation for understanding the spatial and temporal patterns of water

exchange in the hyporheic zones near the coast of Erhai Lake and for studying the mechanisms of nitrogen migration associated with surface water-groundwater exchanges in this area. Additionally, six groundwater sampling points (Points 1–6 in Figure S1) were selected to analyze nitrogen concentration distribution characteristics in various wells and surface waters.

Air temperature significantly effects the temperature of the riverbed in the hyporheic zone, causing seasonal and diurnal variations. These variations also reflect the characteristics of water exchange in the hyporheic zone. The settings for the temperature sensor are presented in the supporting information (Section 1).

This long-term observation captured the dynamic water exchange in the hyporheic zone of Dali Taoxi, including wet, dry, and flood periods, covering varied hydrological scenarios and the dynamics of hyporheic exchange. Throughout the monitoring period, diurnal fluctuations in the riverbed temperature profile were closely mirroring significant diurnal changes in air temperature. Vertically, the differences in temperature amplitude at various depths were more pronounced than the phase differences, highlighting the complexity of heat transfer and water exchange in the hyporheic zone. Based on one-dimensional transient vertical infiltration flux in saturated porous media (Fig. 4), the dynamics of water exchange beneath the riverbed at various depths were depicted employing the Hatch Amplitude method in the VFLUX2 program. The detailed analysis of each part of Fig. 4 is presented in the supporting information (Section 2).

2.3 Laboratory experiment

2.3.1 Experimental design and process

The experiments were conducted in a polymethylmethacrylate rectangular horizontal open box, measuring 0.1 meters in width, 0.6 meters in depth, and 2.4 meters in length, at the Hydrogeology Laboratory of Kunming University of Science and Technology (Figure S7). The sandbox was filled with material sourced directly from the vegetable planting areas on the alluvial fan lacustrine deposits in Dali, which were loess on top and sandy loam beneath. The sandbox was equipped with 55 stainless steel taps distributed on the front and sides; the four rows on the front primarily served as sampling points, while the two rows on the sides were mainly used to adjust the water head height. All tap valves were controllable.

The specific settings of the sandbox are presented in the supporting information (Section 3). The models and suggestions of the auxiliary analytical instruments used in the experiment are listed in Table S4.

2.3.2 Laboratory hyporheic exchange tracer experiment

After filling the sandbox, pure water was continuously injected through an inlet on the left side of the sandbox, elevated at 10 centimeters, to closely observe the advancing wetting front. Four days later, the emergence of water at an outlet at a height of 10 centimeters on the right side indicated that the aquifer

was saturated to a depth of 10 centimeters. Subsequently, pure water was injected through the inlet to saturate the soil layers at depths of 20 centimeters and 30 centimeters, simulating a 30-centimeter-high water table during the dry season.

Common office red ink was selected as the tracer for the experiment. After saturating the aquifer, the dye was injected when the water table was 30 centimeters representing the dry season scenario. Red dye was continuously injected along the top left side close to the inner wall of the sandbox until red dye appeared at the outlet. Photographs were taken at the same location every 24 hours to document the changes in the pollution plume.

For the rainy season, the water table was raised to a depth of 40 centimeters. Office-use blue-black ink was chosen as the tracer. The dye was continuously injected until it ceased to emerge from the outlet. The rainy season tracer experiment demonstrated that most of the irrigation water in the agricultural planting area infiltrated into the sandy loam below, flowing downstream to the outlet with the base flow and predominantly entering the circum-lake sewage interception engineering horizontally. The process of pollutant transmission is shown in the supporting information (Section 4).

2.3.3 Nitrogen transport tracer tests

In this region, the typical use of NPK compound fertilizer features a nitrogen content that generally ranges from 15% to 30%. Select a median value, an NPK fertilizer with a nitrogen content of 22.5% would consist of approximately 13.5% ammonium nitrogen and 10% nitrate nitrogen. Tap water was used as the solvent with ammonium nitrogen and nitrate nitrogen in a 1:1 ratio, each at a concentration of 10 mg/L. The experiment involved drip irrigating this solution onto the soil surface to simulate the infiltration process of fertilizers in agricultural planting areas. The solution was immediately used, dispensed by a fixed-rate drip irrigation device at 0.5 mL per minute, over a period of 25 days.

To minimize experimental errors, the sandbox was continuously infused with pure water to simulate the natural conditions of an aquifer. The water table was maintained at a depth of 40 cm and below, simulating the groundwater system during the rainy season under natural conditions. For testing ammonia nitrogen and nitrate nitrogen, a spectrophotometer was used. The specific testing method is given in the supporting information (Section 5).

3 Results and Discussion

3.1 Vertical distribution characteristics of nitrogen in field investigation

3.1.1 Vertical distribution characteristics of nitrogen during the wet season

In the field sampling process, while arranging temperature sensors, water samples were taken from various depths of the riverbed at the test site to analyze the stability of the water flow. Two days later, on April 17, 2023, water samples were collected once the flow had stabilized, for on-site testing to derive average values for discussion and analysis. The ammonia nitrogen and nitrate nitrogen levels in the water samples were measured using a HACH DR1900 spectrophotometer; ammonia was tested using the Nessler reagent method and nitrate using the cadmium reduction method. Dissolved oxygen measurements were conducted using the Leici Dissolved Oxygen Meter JPB-607A.

During the wet season, the concentrations of ammonia nitrogen and nitrate nitrogen at the river surface were recorded at 0.15 mg/L and 0.12 mg/L, respectively. The riverbed of Taoxi consists of gravel with a median particle size of approximately 65 millimeters, the river flow rate was 0.3038 m^3/s. The gravel has a relatively weak adsorption capacity for ammonia nitrogen and nitrate nitrogen. During the wet season, the river flows swiftly downstream. Although the levels of dissolved oxygen are higher, the effects of nitrification and denitrification are not significant due to the short residence time of the water.

Table S1 and Fig. 5(a) indicates that during the wet season, the average hyporheic flux at a depth of 0.2 m was $2.9\times10^{-5} L/m^2 \cdot s$, second only to the 0.1 m depth, which exhibited the highest coefficient of variation. This suggests that the hyporheic flux is most active within the vertical profile. At this depth, the concentration of ammonia nitrogen is significantly higher than that of nitrate nitrogen. This is because the increased river flow enhances water aeration, the elevated hyporheic flux carries this oxygen deeper into the sediments, which in turn raises the levels of dissolved oxygen. thereby accelerating the conversion of ammonia nitrogen to nitrate nitrogen. As depth increases to 0.425 meters, the average hyporheic flux drops to $7.00\times10^{-6} L/m^2 \cdot s$, approximately a quarter of that at 0.2 meters, due to poorer oxygen diffusion and consumption by microorganisms in the sediment, which leads to reduced levels of dissolved oxygen. Consequently, the concentration of ammonia nitrogen surges at this depth, while the concentration of nitrate nitrogen remains relatively unchanged from the 0.2 meters depth.

There are two primary reasons for this pattern: firstly, although the hyporheic flux at 0.4 meters is lower compared to shallower sediment layers, the flux direction remains consistent, continuously replenishing this site, which allows pollutants to accumulate at this depth. Therefore, the concentration of ammonia nitrogen at this depth is approximately 4.6 times higher than at 0.2 meters. Secondly, the concentration of nitrate nitrogen decreases by about 30% compared to the 0.2 meters depth. As the depth increases, the poorer oxygen diffusion in the water results in lower dissolved oxygen concentrations, and the riverbed sediments provide a more stable environment that is conducive to the formation of stable anaerobic microbial communities. Through dissimilatory reduction, nitrate nitrogen is converted back to ammonia nitrogen. Optimal denitrification activity occurs under near-anoxic conditions, typically when dissolved oxygen levels are less than 0.5 mg/L. However, some denitrification processes can occur under microaerophilic conditions, where dissolved oxygen levels are low but still detectable, approximately 0.2-2 mg/L (Naranjo et al., 2015).

3.1.2 Vertical distribution characteristics of nitrogen during dry season

This study, conducted on May 4, 2023, during this period, both the river surface and the sediments at a depth of 0.1 meters were dry due to the cessation of surface water inflow and intense evaporation. The lack of new water sources and the negative hyporheic flux, indicative of upward evaporation, led to a significant reduction in dissolved oxygen at 0.2 meters. This created an unstable anaerobic environment in the waterlogged soil or gravel, resulting the reduction to ammonia nitrogen.

Figure 5(b) indicates that at this location, dissimilatory reduction resulted in an ammonia nitrogen concentration approximately 2.7 times higher than that observed during the wet season. In contrast, the nitrate nitrogen concentration decreased to 59% of its wet season level. At a depth of 0.4 meters, where the hyporheic flux was relatively stable (decreasing from 7.00×10^{-6} L/m^2·s to 5.03×10^{-6} L/m^2·s), the dissolved oxygen content decreased slightly. However, the concentrations of ammonia nitrogen and nitrate nitrogen at this depth remained similar to those in the wet season, continuing to reflect an anaerobic environment dominated by dissimilatory reduction.

During the wet season, the shallow sediment layer (0.2 meters deep) not only transported abundant dissolved oxygen due to significant hyporheic flux but also carried dissolved ammonia and nitrate nitrogen from the surface water. This influx of oxygen facilitated nitrification, resulting in a higher concentration of nitrate nitrogen than ammonia nitrogen at this depth. However, during the dry season, the scenario reversed entirely: the riverbed dried up, and no new water flow replenished the dissolved oxygen in the sediment, leading to an anaerobic environment where dissimilatory reduction predominated and increased the ammonia nitrogen concentration relative to nitrate nitrogen (Zhu et al., 2023). In deeper riverbed sediments (0.4 meters deep), although the hyporheic flux was smaller, it remained relatively unaffected by environmental changes due to continuous replenishment from upper water layers. This steady supply not only maintained a higher ammonia nitrogen concentration but also supported ongoing dissimilatory reduction under anaerobic conditions, further transforming nitrate nitrogen into ammonia nitrogen. Previous research suggests that while nitrification primarily occurs in the shallow layers of the hyporheic zone, denitrification is more prevalent at the bottom of the sediment layer (Shuai et al., 2017).

The above analysis indicates that while the riverbed's hyporheic filtration system can somewhat mitigate nitrate nitrogen pollution of groundwater from river water, its effectiveness is compromised by dissimilatory reduction reactions in the riverbed sediments under anaerobic conditions, leading to increased ammonia nitrogen concentrations. This not only diminishes the purifi cation capability of the hyporheic filtration system but also exacerbates groundwater contamination. Therefore, the potential negative impact of rising ammonia nitrogen concentrations on groundwater quality must be carefully considered.

3.2 Migration characteristics of nitrogen in the experiment

3.2.1 Migration characteristics of ammonia nitrogen in the sandbox section

The experimental setup to this study is depicted in the Figure S8. Initial concentrations were set at 10 mg/L for both ammonia and nitrate nitrogen to simulate fertilizer leaching. Sampling points A1 through D4, totaling 24, were analyzed every five days. As illustrated in Figs. 6, the collected data was processed and analyzed using kriging interpolation.

As indicated in Fig. 6(A) and Fig. 7, based on the results of the indoor drip irrigation experiment, the sandbox was divided into three regions for analysis:

Region 1: Groundwater Seepage Area (A1, A2, B2, B3, C2, C3, D4)

The soil in the sampling area contains significant nitrogen levels due to years of fertilizer application. Previous pollution tracer experiments and drip irrigation tests have outlined the approximate migration path of pollutants from A1 to D4.

In the initial stages of the experiment, ammonia nitrogen concentrations at the sampling points A1 and A2, situated at soil profile depths of 10 centimeters and 20 centimeters respectively, increased rapidly. By the fifth day, concentrations were reached 2.9 mg/L and 3.3 mg/L, respectively. Similarly, concentrations at B2 and B3 peaked at 2.7 mg/L and 1.9 mg/L, respectively. At C3, the concentration increased to 1.4 mg/L, which facilitated by the soil's infiltration capabilities. In contrast, sampling points in column D, which contained inherent nitrogen due to the fill soil, exhibited a reduction in ammonia nitrogen concentration from the initial measurements by 0.5 mg/L to 0.7 mg/L. This change occurred because the pollutants had not yet reached column D, and the continuous replenishment by base flow along with the leaching effect of pure water caused the inherent ammonia nitrogen in the soil particles to dissolve or desorb and be carried away. Extending the leachate injection time from 5 to 20 days resulted in a pollution concentration curve that gradually advanced along the seepage path. By the 20th day, the highest ammonia nitrogen concentration was observed at the C2 sampling point, reaching 16.7 mg/L. This was followed by B2 at 15.6 mg/L, and A1 and A2, where concentrations increased to 7.5 mg/L and 5.3 mg/L.

From day 0 to day 20, the concentration of ammonia nitrogen along the seepage path exhibited a decreasing trend. This phenomenon primarily arises due to the charged surfaces of soil solids, which result from chemical bond breaks, lattice defects, and isomorphous substitution (Nommik and Vahtras, 1982). These charges allow the solids to maintain equilibrium by adsorbing charged ions. Mineral lattices carry a net negative charge, which facilitates the adsorption of cations. In the soil where both NH_3 and NH_4^+ exist freely, cation adsorption significantly influences their vertical distribution. Negatively charged soil colloids can absorb considerable amounts of ammonia nitrogen, impeding its downward migration and resulting in a gradual reduction in concentration from the top to the bottom of the soil profile.

During the evaluation of ammonia nitrogen concentrations in the sandbox, two sampling points, B2 and C2, recorded abnormally high concentrations. There are two primary reasons for this: Firstly, B2 and C2 are situated directly beneath and to the left of the circum-lake sewage interception engineering, respectively. During the injection of the pollutant solution, a significant portion was adsorbed by soil particles through surface runoff, infiltration, and adsorption processes. Influenced by capillary forces and gravity, this portion of the pollutant solution moved erratically within soil pores, gradually accumulating while dissolving and displacing the ammonia nitrogen initially present in the soil, which was eventually accumulated near the circum-lake sewage interception engineering. The lack of an impermeable barrier at the base of this structure allowed these pollutants to seep back into the groundwater under gravitational influence, causing dual contamination at the B2 and C2 sampling points leading to continuously rising ammonia nitrogen concentrations. Secondly, over time, the ammonia nitrogen concentrations at upstream sampling points A1 and A2 were lower than those downstream. This is attributed to the continuous conditions of pond percolation, where soil moisture rapidly percolated downward, reducing the solute concentration through base flow leaching.

Region 2: Non-groundwater Seepage Area (A4, B4, C1, C4, D2, D3)

At the sampling points A4, B4, and C4, located near the bottom of the sandbox, the response to pollutant penetration was relatively slow, with the highest ammonia nitrogen concentrations observed on the 20th day of the experiment. This pattern arose because these points are distant from the pollution source and main flow paths. Only a minimal amount of pollutants migrated to the sandbox's bottom through soil pores, influenced by gravity, infiltration, and adsorption actions. Most pollutants, influenced by base flow replenishment, continued to move laterally, migrating from A4 to B4 and C4, and eventually converging at the D4 sampling point. This resulted in a progressively increasing trend in pollutant concentrations laterally along the base flow streamlines.

The C1 sampling point, being far from both the circum-lake sewage interception engineering and the pollution injection points, showed little change in ammonia nitrogen concentration. At D2, the ammonia nitrogen concentration reached its lowest value within the first five days of the experiment and peaked on the 20th day, displaying relatively minor fluctuations. This minor increase is primarily because the sampling point is also distant from the main flow path and is influenced by the water at the upstream D3 sampling point rising through capillary action. However, since the distance from D3 to the outlet is much shorter than from C2 to the outlet, the water at D3 flows out quickly along the groundwater. This results in weaker capillary action at D3 compared to C1, thus causing much smaller changes in ammonia nitrogen concentration at D2 compared to C1.

Region 3: Surface Water Body B1 around the Lake Sewage Interception Engineering, D1 Erhai Lake

As the total amount of pollutants increased during the drip irrigation process, the ammonia nitrogen concentration in the circum-lake sewage interception engineering exhibited a continuous upward trend, escalating from a background value of 0.2 mg/L to 5.9 mg/L by the 25th day. In this experiment, which used dissolved compound fertilizer as the pollution source, nitrogen loss primarily occurred in primarily

dissolved form. According to Jani et al. (2020), organic nitrogen are the predominant forms of soluble nitrogen lost in runoff, indicating that nitrogen loss through runoff water is significantly higher than through runoff carrying sediment.

The D1 sampling point, used in this experiment to simulate Erhai Lake, showed no significant change in ammonia nitrogen concentration under continuous pollution drip irrigation. This outcome is likely due to the sandbox model's scale limitations, which cannot accurately replicate the depth and area of Erhai Lake, most pollutants flowed out through the sandbox's bottom outlet. In the real environment, during the rainy season in the Dali area, the pollutants from agricultural areas ultimately flow into Erhai Lake.

3.2.2 Migration characteristics of nitrate nitrogen in the sandbox section

In Fig. 6(B) and Fig. 8, based on the results of the indoor drip irrigation experiment, we can discuss nitrate nitrogen by dividing the sandbox into three regions:

Region 1: Groundwater Seepage Area (A1, A2, B2, B3, C2, C3, D4)

This region exhibits the most significant changes in nitrate nitrogen concentration. Unlike the distribution of ammonia nitrogen, the highest concentration of nitrate nitrogen was observed in the shallow soil at sampling point A1, where it continuously rose to a peak of 28.4 mg/L on the 25th day.

From days 0 to 10, the concentration of nitrate nitrogen consistently increased along the seepage path. Due to the fact that soil colloids, which carry a negative charge, adsorb very little of the negatively charged nitrate nitrogen. During the process of water flowing downward, more nitrate nitrogen is leached away.. Although soil surfaces also carry some positive charges, these charges are insufficient to effectively adsorb the large volume of negatively charged nitrate nitrogen. Thus, nitrate nitrogen increased with with soil depth, thereby increasing the risk of nitrogen pollution in the aquifer groundwater (Li et al., 2023). From this analysis, it is clear that the concentration of nitrate nitrogen at different soil profile depths is greatly influenced by hydrodynamic conditions, and over time, the trend of nitrate nitrogen enriching downward becomes increasingly evident.

Region 2: Non-groundwater Seepage Area (A4, B4, C1, C4, D2)

At sampling point C1, both nitrate and ammonia nitrogen concentrations showed a continual upward trend over time, nitrate nitrogen increasing at a faster rate. This phenomenon is proximity of the point to the surface, where the upper soil layer is an aerobic environment. Lateral seepage from point B1 near the circum-lake sewage interception engineering brings dissolved oxygen, facilitating the rapid conversion of ammonia nitrogen or ammonium ions to nitrite nitrogen and ultimately to nitrate nitrogen. This nitrification process, primarily carried out by two types of autotrophic bacteria (ammonia-oxidizing and nitrite-oxidizing bacteria), a similar process occurred at sampling point D2, thus resulting in higher nitrate nitrogen content compared to ammonia nitrogen.

At points A4, B4, and C4, located at the bottom of the sandbox and far from the seepage points, the concentration of nitrate nitrogen initially increased but then continuously decreased. With its negative charge, is not adsorbed or retained by soil colloids, allowing it to quickly percolate to the bottom of the sandbox. The downward movement of nitrate nitrogen through the soil layers is influenced by microbial activity.

Region 3: Surface Water Body B1 around the Lake Sewage Interception Engineering, D1 Erhai Lake

At the B1 circum-lake sewage interception engineering site, the concentration of nitrate nitrogen consistently increased with the ongoing injection of pollutants, rising from 0.1 mg/L on day 0 to 4.2 mg/L by day 25. In contrast, the concentration of ammonia nitrogen remained consistently lower than that of nitrate nitrogen, despite both pollutants being initially injected at a concentration of 10 mg/L. This suggests that water percolation facilitates the activity of soil microbes, which then convert ammonia nitrogen to nitrate nitrogen through the process of nitrification. At D1, the concentrations of nitrate nitrogen remained similar to those of ammonia nitrogen, consistently at lower levels. This is because the upstream migration of pollutants along the seepage path minimally impacts this location.

From the time-series graphs of total ammonia nitrogen and total nitrate nitrogen concentrations shown in Figure S10, it can be deduced that the concentration of ammonia nitrogen in the leachate consistently remained lower than that of nitrate nitrogen. This also indirectly indicates that ammonia nitrogen undergoes cationic adsorption in the sandbox, resulting in consistently higher concentrations of nitrate than ammonia in the leachate. In contrast, the adsorption of nitrate nitrogen by soil particles is weaker. The groundwater nitrate content increases with increased stream water infiltration time, corroborating findings from previous studies by Xia et al. (2024).

3.2.3 Mechanism of nitrogen transport and transformation

By creating a stacked graph of ammonia and nitrate nitrogen concentrations, we can visually observe the variations in these concentrations over time at various locations and depths within the sandbox (see Fig. 9). This comparison of ammonia and nitrate nitrogen concentrations reveals several key observations about the nitrogen migration process:

A. Nitrification

Throughout the experiment, particularly at sampling points closest to the surface soil (A1, C1), a sharp increase in nitrate nitrogen concentration is observed, which is higher than at other points. Since the injected pollutant solution contained concentrations of both ammonia nitrogen and nitrate nitrogen at 10 mg/L, this phenomenon is attributed to nitrification. This process occurs in two stages:

1. First stage:

Under the influence of nitrosifying bacteria, ammonium ions (NH_4^+) is oxidized to nitrate nitrogen (NO_3^-) according to the following reaction:

$$NH_4^+ + \frac{3}{2O_2} \rightarrow\ NO_2^- + H_2O + 2H^+ - \Delta\ F\Delta\ F = 278.42KJ$$

1

2. Second stage:

The nitrate nitrogen formed undergoes further oxidation by nitrifying bacteria and microbes, forming NO_3^-, as shown in the reaction:

$$NO_2^- + \frac{1}{2O_2} \rightarrow\ NO_3^- - \Delta\ F\ (\Delta\ F = 72.27KJ)$$

2

In the shallow soil, the pollutant solution ensures a relatively high dissolved oxygen concentration. The dissolved oxygen in the infiltrating liquid is continuously consumed due to nitrification, thus the DO concentration in the leachate from the A1 sampling point continuously decreases. Additionally, the pH time curve at the A1 shows a consistent decline(Figure S9(B)), as the nitrification reaction generates hydrogen ions, making the process acid-producing. Combined with the measured values of dissolved oxygen, it can be concluded that there is a variation in concentration with depth, showing a tendency to decrease with increasing depth.

B. Dissimilatory Reduction

During the initial 20 days of the experiment, with the continuous introduction of nitrogenous pollutants, the concentration of ammonia nitrogen in the leachate from soil depths ranging from 10 to 40 centimeters within the sandbox exhibited an overall upward trend, the concentration of nitrate nitrogen in the leachate displayed a stable decline. Notably, the concentration of nitrate nitrogen in the effluent was lower than that in the inflow, a phenomenon not attributable to the denitrification process. During this phase, hydrodynamic actions and dissimilatory reduction processes were predominantly involved. Dissimilatory reduction, a microbial process, involves the reduction of nitrate nitrogen to ammonium nitrogen, resulting in a decrease in nitrate nitrogen content. The reaction for dissimilatory reduction is:

$$NO_3^- + 10H^+ + 8e^- = NH_4^+ + 3H_2O$$

3

In this reaction, nitrate nitrogen serves as the electron acceptor, and in the presence of microbes and an anaerobic environment, dissimilatory reduction of nitrate nitrogen to ammonium ions occurs. Importantly, the presence of organic nitrogen and ammonium ions does not inhibit this process. The occurrence of dissimilatory reduction in related systems can be explained by the following factors:

1. Under saturated conditions in the aquifer, the soil often remains in an anaerobic state, which is a favorable and necessary condition for the conversion of nitrate nitrogen to ammonium nitrogen.
2. Research by various scholars, has demonstrated that added labeled nitrogen ($^{15}NO_3^-$) can be converted to $^{15}NH_4^+$ under certain conditions. This conversion is not limited to soil but also occurs in sediments, where the transformed $^{15}NH_4^+$ is considered a product of dissimilatory reduction (Bengtsson and Annadotter, 1989).
3. Dissimilatory reduction and denitrification are two parallel processes that consume nitrate nitrogen and compete with each other. When the dissimilatory reduction process is enhanced, denitrification is relatively suppressed because the primary transformation of nitrate nitrogen through dissimilatory reduction becomes ammonium ions, thus reducing the nitrate nitrogen available for denitrification. It has been found that the rate of denitrification may be three times lower than that of dissimilatory reduction, suggesting that dissimilatory reduction may be the dominant process of nitrate nitrogen transformation under certain conditions. Therefore, promoting dissimilatory reduction can be an effective strategy for nitrate removal. The ammonia ammonium ions produced by the dissimilatory reduction process, under alkaline conditions, does not easily volatilize and can be directly used as a nitrogen source for crops. This not only helps reduce nitrogen loss in fields but also enhances the absorption and utilization efficiency of nitrogen by crops, positively impacting agricultural production and environmental protection.
4. As shown in Figure S10, it is observed that the total concentration of these compounds in the effluent is slightly higher compared to the inflow. During this process, the total amount of nitrogen remains constant, with only the form of changing. Nitrate nitrogen is transformed into ammonia nitrogen through dissimilatory reduction, resulting in similar total concentrations of ammonia and nitrate nitrogen in the effluent compared to the inflow. The intermediate in the transformation from nitrate to ammonia nitrogen is nitrite, which is unstable in nature, due to the varying rates of different reactions, the distribution of nitrite content lacks regularity.

C. Denitrification

Between days 20 and 25 of the experiment, the concentration of ammonia nitrogen at the D4 outlet ceased increasing, while the concentration of nitrate nitrogen decreased, falling below the levels near the inflow. This reduction can be attributed to the soil at a depth of 10–40 cm in the sandbox meeting the essential conditions required for denitrification, including: (1) pollutants serving as reaction substrates; (2) the presence of denitrifying bacteria; (3) sufficient electron acceptors; (4) an anaerobic environment. The denitrification process then occurs, leading to the reduction of nitrate nitrogen, as illustrated by the following equation:

$$2C\,(carbon\ source) + 2\mathrm{NO}\backslash:_3^- + \mathrm{H_2O} = 2\mathrm{HCO}\backslash:_3^- + \mathrm{N_2O}\uparrow\backslash:$$

4

Under anaerobic conditions, nitrate nitrogen acts as the electron acceptor and is processed through denitrification when abundant denitrifying microbes and a sufficient carbon source are present. During percolation in riverbeds, the factors contribute to denitrification can be found in the supporting information(Section 6).

4 Summary and Conclusions

This study examines field investigations and temperature monitoring of riverbeds near the area of the lake sewage interception engineering, augmented by an analysis of hyporheic flux, to explore patterns of nitrogen transformation and migration at various depths within the riverbed. Monitoring of nitrogen in both groundwater and surface water in agricultural areas surrounding the sewage interception system, alongside indoor physical model experiments, has facilitated an analysis of the mechanisms driving nitrogen migration and transformation within the interface of groundwater and surface water in the area. The following main conclusions have been reached:

1. Hyporheic flux is closely associated with seasonal variations in river levels. Typically, during the wet season, the hyporheic flux is positive, suggesting that surface water is replenishing groundwater, whereas the amplitude of deeper hyporheic flux diminishes with depth. During the dry season, hyporheic flux at a depth of 0.15 m often becomes negative.
2. In the wet season, the inflow of hyporheic flux into the riverbed not only transports a significant amount of dissolved oxygen to the shallow sediment layer (0.2 meters deep) but also facilitates the accumulation of ammonia and nitrate nitrogen in the water of this depth's hyporheic zone. At a deeper layer (0.4 meters deep), regardless of the season, the continuous influx of hyporheic flux from upper sediments leads to the accumulation of ammonia nitrogen, and under anaerobic conditions, dissimilatory reduction transforms nitrate nitrogen to ammonia nitrogen.
3. Indoor sandbox experiments simulated the movement of water from the lake sewage interception engineering area discharging into Erhai Lake. During the rainy season, when the groundwater level is higher, irrigation water in the agricultural planting area intersects with the base flow at a depth of 0.1 m one day after infiltration, directing groundwater towards the sewage interception engineering. In the dry season, irrigation water intersects with the base flow at a depth of 0.2 m three days after infiltration; most of the water bypasses the sewage interception engineering, with only a small fraction flowing horizontally into it and Erhai Lake.
4. Sandbox nitrogen migration tracer experiments reveal that in shallow soils, nitrogen transformation predominantly occurs through nitrification, whereas in deeper soils, it is governed by denitrification and dissimilatory reduction. During the early phase of the experiment (0–20 days), dissimilatory reduction results in decreasing nitrate concentrations and increasing ammonia concentrations. In the later stages of the experiment (20–25 days), denitrification significantly reduces nitrate concentrations in the effluent. Lastly, the content of nitrate in groundwater increases with the duration of pond or drain infiltration near the upstream of the lake.

This study examines the regional-scale hydrogeological survey discrepancies and integrates laboratory-scale studies on percolation and nitrogen migration and transformation mechanisms to discuss the contribution of near-lake sewage interception engineering to lake eutrophication. Overall, the hydraulic gradient between the water bodies of the sewage interception engineering and Erhai Lake facilitates hyporheic exchange and base flow replenishment. Simultaneously, the accumulated and enriched nitrogen pollutants in the sedimentary deposits along the lake provide a continuous source of pollution through hyporheic exchange. In future studies, we aim to further explore the interactions between surface water and groundwater and their nitrogen cycling mechanisms under conditions of hydrodynamic, biological, and hydrogeochemical coupling, particularly on the west side of Erhai Lake. This research will include different nitrogen supply sources and scale conditions under surface water-groundwater cycling mechanisms, and their contributions to the leaching and migration transformation mechanisms at various depths and concentrations. It will also examine the original nitrogen point, line, and area sources of pollution and their contributions to the eutrophication of Erhai Lake. Although the implementation of sewage interception engineering around Erhai Lake has controlled non-point source pollution from entering the lake directly, the increase in the groundwater head in the lake's shore zone post-implementation raises concerns. The mechanisms of hyporheic exchange that replenish Erhai Lake's surface water, along with the leaching and migration mechanisms of existing nitrogen pollution sources in the groundwater from the village's lake sedimentary layers into Erhai Lake, remain unclear.

Declarations

Funding

This study was supported by he National Natural Science Foundation of China (Nos. 42167052 and 42267063) and the Yunnan Province "Xing Dian talent Support Plan" young talents (Nos. KKXX202421024).

Author Contribution declaration

Ronggao Qin: Writing, Review and editing, Funding acquisition, Project administration.

Haoyi Li: Conceptualization, Methodology, Investigation, Main experiment and research, Writing- original draft, Drawn various illustrations.

Wan Xu: Literature search and classification, Drawn various illustrations.

Ciming Kong: Supervision.

Yiming Xie: Investigation

Guangzhu Cao: Literature search and classification, Supervision.

Ruoyu Mao:Experiment

Yi Qiang: Literature search and classification.

Yanfeng Lu: Validation.

Author email

Ronggao Qin <qinronggao@126.com>

Haoyi Li <931055452@qq.com>

Wan Xu <2435119419@qq.com>

Ciming Kong <1035417670@qq.com>

Yiming Xie <826059707@qq.com>

Ruoyu Mao <784941183@qq.com>

Yi Qiang <462766753@qq.com>

Yanfeng Lu <136361052@qq.com>

Acknowledgments

We thank the anonymous reviewer and the Editor for their helpful and constructive comments on an earlier version, which have led to significant improvement of this manuscript.

References

1. Assa, B.G., Bhowmick, A., Cholo, B.E., 2024. Assessing Nitrate Leaching and Runoff Coefficients in the Dynamic Interplay of Seasonal Crop Biomass: A Study of Surface and Groundwater Nitrate Contamination in the Bilate Cropland Watershed. Environmental Advances, 16: 100528.
2. Basilio Hazas, M., Ziliotto, F., Lee, J., Rolle, M., Chiogna, G., 2023. Evolution of plume geometry, dilution and reactive mixing in porous media under highly transient flow fields at the surface water-groundwater interface. J. Contam. Hydrol., 258: 104243.
3. Bengtsson, G., Annadotter, H., 1989. Nitrate Reduction in a Groundwater Microcosm Determined by 15N Gas Chromatography-Mass Spectrometry. Appl Environ Microb, 55(11): 2861–2870.
4. Boano, F. et al., 2014. Hyporheic flow and transport processes: Mechanisms, models, and biogeochemical implications. Rev. Geophys., 52(4): 603–679.

5. Bouchez, C., Cook, P.G., Partington, D., Simmons, C.T., 2021. Comparison of Surface Water-Groundwater Exchange Fluxes Derived From Hydraulic and Geochemical Methods and a Regional Groundwater Model. Water Resour. Res., 57(3): e2020WR029137.
6. Briggs, M.A., Lautz, L.K., McKenzie, J.M., Gordon, R.P., Hare, D.K., 2012. Using high-resolution distributed temperature sensing to quantify spatial and temporal variability in vertical hyporheic flux. Water Resour. Res., 48(2): W02527.
7. Chen, C., Zeng, L., 2015. Using the level set method to study the effects of heterogeneity and anisotropy on hyporheic exchange. Water Resour. Res., 51(5): 3617–3634.
8. Chow, R., Parker, B.L., Steelman, C.M., Thoms, A., Nowak, W., 2021. How Do Fractures Influence Hyporheic Exchange in Sedimentary Rock Riverbeds? Water Resour. Res., 57(7): e2020WR028476.
9. Cui, R. et al., 2023. Nitrogen in soil, manure and sewage has become a major challenge in controlling nitrate pollution in groundwater around plateau lakes, Southwest China. J. Hydrol., 620: 129541.
10. Earon, R., Riml, J., Wu, L., Olofsson, B., 2020. Insight into the influence of local streambed heterogeneity on hyporheic-zone flow characteristics. Hydrol. J., 28(8): 2697–2712.
11. Gao, C., Kong, J., Wang, J., Chen, W., 2024a. Nitrate fate in coastal unconfined aquifers influenced by preferential flows. Frontiers in Marine Science, 11.
12. Gao, S., Zheng, T., Zhang, B., Fang, Y., Zheng, X., 2024b. Combined effects of aquifer heterogeneity and subsurface dam on nitrate contamination in coastal aquifers. J. Environ. Manage., 351: 119740.
13. Gomez-Velez, J.D., Krause, S., Wilson, J.L., 2014. Effect of low-permeability layers on spatial patterns of hyporheic exchange and groundwater upwelling. Water Resour. Res., 50(6): 5196–5215.
14. Gooseff, M.N., 2010. Defining Hyporheic Zones – Advancing Our Conceptual and Operational Definitions of Where Stream Water and Groundwater Meet. Geography Compass, 4(8): 945–955.
15. Gordon, R.P., Lautz, L.K., Briggs, M.A., McKenzie, J.M., 2012. Automated calculation of vertical pore-water flux from field temperature time series using the VFLUX method and computer program. J. Hydrol., 420–421: 142–158.
16. Guo, Z., Chen, K., Yi, S., Zheng, C., 2023. Response of groundwater quality to river-aquifer interactions during managed aquifer recharge: A reactive transport modeling analysis. J. Hydrol., 616: 128847.
17. Hare, D.K., Helton, A.M., Johnson, Z.C., Lane, J.W., Briggs, M.A., 2021. Continental-scale analysis of shallow and deep groundwater contributions to streams. Nature Communications, 12(1): 1450.
18. Hingst, M.C. et al., 2023. Surface Water-Groundwater Connections as Pathways for Inland Salinization of Coastal Aquifers. Groundwater, 61(5): 626–638.
19. Jafari, T., Kiem, A.S., Javadi, S., Nakamura, T., Nishida, K., 2021. Fully integrated numerical simulation of surface water-groundwater interactions using SWAT-MODFLOW with an improved calibration tool. Journal of Hydrology: Regional Studies, 35: 100822.
20. Jani, J., Yang, Y.-Y., Lusk, M.G., Toor, G.S., 2020. Composition of nitrogen in urban residential stormwater runoff: Concentrations, loads, and source characterization of nitrate and organic

nitrogen. Plos One, 15(2): e0229715.

21. Ji, N., Wang, S., Zhang, L., 2017. Characteristics of dissolved organic phosphorus inputs to freshwater lakes: A case study of Lake Erhai, southwest China. Sci. Total Environ., 601–602: 1544–1555.
22. Jin, G. et al., 2022. Transport of Phosphorus in the Hyporheic Zone. Water Resour. Res., 58(3): e2021WR031292.
23. Laube, G., Schmidt, C., Fleckenstein, J.H., 2018. The systematic effect of streambed conductivity heterogeneity on hyporheic flux and residence time. Adv. Water Res., 122: 60–69.
24. Lautz, L.K., 2010. Impacts of nonideal field conditions on vertical water velocity estimates from streambed temperature time series. Water Resour. Res., 46(1): W01509.
25. Ledford, S.H., Briggs, M., Glas, R., Zimmer, M.A., 2022. Connecting diverse disciplines to improve understanding of surface water-groundwater interactions. Journal of Hydrology X, 17: 100141.
26. Lee, A., Aubeneau, A.F., Cardenas, M.B., Liu, X., 2022. Hyporheic Exchange Due to Cobbles on Sandy Beds. Water Resour. Res., 58(1): e2021WR030164.
27. Lewandowski, J., Rosenberry, D.O., Meinikmann, K., 2024. Groundwater–Lake Interfaces, Ecohydrological Interfaces, pp. 103–122.
28. Li, A., Aubeneau, A.F., Bolster, D., Tank, J.L., Packman, A.I., 2017. Covariation in patterns of turbulence-driven hyporheic flow and denitrification enhances reach-scale nitrogen removal. Water Resour. Res., 53(8): 6927–6944.
29. Li, H. et al., 2023. Effects of irrigation and nitrogen application on NO3–N distribution in soil, nitrogen absorption, utilization and translocation by winter wheat. Agricultural Water Management, 276: 108058.
30. Li, Z. et al., 2016. Using multiple combined analytical techniques to characterize water extractable organic nitrogen from Lake Erhai sediment. Sci. Total Environ., 542: 344–353.
31. Lin, S.-S., Shen, S.-L., Zhou, A., Lyu, H.-M., 2020. Sustainable development and environmental restoration in Lake Erhai, China. Journal of Cleaner Production, 258: 120758.
32. Lin, S.-S., Shen, S.-L., Zhou, A., Lyu, H.-M., 2021. Assessment and management of lake eutrophication: A case study in Lake Erhai, China. Sci. Total Environ., 751: 141618.
33. Lin, Y., Lu, C., Wu, C., Liu, B., Shu, L., 2023. Hyporheic exchange and nitrogen cycle processes under the dual effects of flooding and heterogeneous streambed. J. Hydrol., 626: 130188.
34. Lotts, W.S., Hester, E.T., 2022. Pipe Dreams: The Effects of Stream Bank Soil Pipes on Hyporheic Denitrification Caused by a Peak Flow Event. Water Resour. Res., 58(4): WR030312.
35. Lu, Z., Yang, X., 2024. Effects of microtopography on patterns and dynamics of groundwater–surface water interactions. Adv. Water Res., 188: 104704.
36. Lutz, S.R. et al., 2020. How Important is Denitrification in Riparian Zones? Combining End-Member Mixing and Isotope Modeling to Quantify Nitrate Removal from Riparian Groundwater. Water Resour. Res., 56(1): e2019WR025528.

37. Marti, E. et al., 2023. Unravelling geological controls on groundwater flow and surface water-groundwater interaction in mountain systems: A multi-disciplinary approach. J. Hydrol., 623: 129786.
38. Marzadri, A., Ciriello, V., de Barros, F.P.J., 2024. Hyporheic Flows in Stratified Sediments: Implications on Residence Time Distributions. Water Resour. Res., 60(1): e2023WR035625.
39. Marzadri, A., Tonina, D., Bellin, A., 2011. A semianalytical three-dimensional process-based model for hyporheic nitrogen dynamics in gravel bed rivers. Water Resour. Res., 47(11): W11518.
40. Monofy, A., Boano, F., 2021. The Effect of Streamflow, Ambient Groundwater, and Sediment Anisotropy on Hyporheic Zone Characteristics in Alternate Bars. Water Resour. Res., 57(1): e2019WR025069.
41. Moore, E.M. et al., 2023. Where the past meets the present: connecting nitrogen from watersheds to streams through groundwater flowpaths. Environ. Res. Lett., 18(12): 124039.
42. Naranjo, R.C., Niswonger, R.G., Davis, C.J., 2015. Mixing effects on nitrogen and oxygen concentrations and the relationship to mean residence time in a hyporheic zone of a riffle-pool sequence. Water Resour. Res., 51(9): 7202–7217.
43. Nelson, A.R. et al., 2019. Heterogeneity in Hyporheic Flow, Pore Water Chemistry, and Microbial Community Composition in an Alpine Streambed. Journal of Geophysical Research: Biogeosciences, 124(11): 3465–3478.
44. Ni, Z., Wang, S., Zhang, M., 2016. Sediment amino acids as indicators of anthropogenic activities and potential environmental risk in Erhai Lake, Southwest China. Sci. Total Environ., 551–552: 217–227.
45. Nommik, H., Vahtras, K., 1982. Retention and Fixation of Ammonium and Ammonia in Soils, Nitrogen in Agricultural Soils. Agronomy Monographs, pp. 123–171.
46. Partington, D. et al., 2023. Where the water goes: Partitioning surface flow and streambed infiltration in an ephemeral river laboratory experiment. J. Hydrol., 626: 130159.
47. Ping, X., Xian, Y., Jin, M., 2023. Effect of Particulate Organic Carbon Deposition on Nitrate Reduction in the Hyporheic Zone. Water Resour. Res., 59(7): e2022WR034253.
48. Pryshlak, T.T., Sawyer, A.H., Stonedahl, S.H., Soltanian, M.R., 2015. Multiscale hyporheic exchange through strongly heterogeneous sediments. Water Resour. Res., 51(11): 9127–9140.
49. Ren, J., Zhuang, T., Wang, F., Dai, J., Wang, J., 2023. Hyporheic exchange law driven by spur dikes: Numerical modeling. J. Hydrol., 618: 129203.
50. Shuai, P., Cardenas, M.B., Knappett, P.S.K., Bennett, P.C., Neilson, B.T., 2017. Denitrification in the banks of fluctuating rivers: The effects of river stage amplitude, sediment hydraulic conductivity and dispersivity, and ambient groundwater flow. Water Resour. Res., 53(9): 7951–7967.
51. Song, X. et al., 2024. Influence of point bars on nitrogen transport and reaction in riparian zones. J. Hydrol., 637: 131388.

52. Suning, L., May, C.T.F., 2018. Impacts of Streambed Heterogeneity and Anisotropy on Residence Time of Hyporheic Zone. Groundwater, 56(3): 425–436.
53. Tajari, M., Omid, M.H., Dehghani, A.A., Ghameshlou, A.N., Boano, F., 2023. Effect of Combined Subsurface Structures and Steps on Hyporheic Exchange. Water Resour. Res., 59(5): e2022WR033991.
54. Valett, H.M., Reinhold, A.M., 2022. Groundwater and Surface Water Interaction. In: Mehner, T., Tockner, K. (Eds.), Encyclopedia of Inland Waters (Second Edition). Elsevier, Oxford, pp. 348–362.
55. Wang, M. et al., 2024a. A triple increase in global river basins with water scarcity due to future pollution. Nature Communications, 15(1): 880.
56. Wang, P. et al., 2023. A parsimonious model for predicting the NO3–-N concentration in shallow groundwater in intensive agricultural areas using few easily accessible indicators and small datasets based on machine learning. J. Hydrol., 619: 129356.
57. Wang, Z. et al., 2024b. How redox gradient potentially influences nitrate reduction coupled with sulfur cycling: A new insight into nitrogen cycling in the hyporheic zone of effluent-dominated rivers. Sci. Total Environ., 915: 170070.
58. Wei, X., Bailey, R.T., Records, R.M., Wible, T.C., Arabi, M., 2019. Comprehensive simulation of nitrate transport in coupled surface-subsurface hydrologic systems using the linked SWAT-MODFLOW-RT3D model. Environmental Modelling & Software, 122: 104242.
59. Wexler, S.K., Hiscock, K.M., Dennis, P.F., 2011. Catchment-Scale Quantification of Hyporheic Denitrification Using an Isotopic and Solute Flux Approach. Environmental Science & Technology, 45(9): 3967–3973.
60. Xia, Y., Xiao, J., Wang, W., Li, Z., 2024. Nitrate dynamics in the streamwater-groundwater interaction system: Sources, fate, and controls. Sci. Total Environ., 918: 170574.
61. Xu, S. et al., 2021. Investigating groundwater-lake interactions in the Laurentian Great Lakes with a fully-integrated surface water-groundwater model. J. Hydrol., 594: 125911.
62. Yifru, B.A., Chung, I.-M., Kim, M.-G., Chang, S.W., 2022. Assessing the effect of urbanization on regional-scale surface water-groundwater interaction and nitrate transport. Sci Rep-Uk, 12(1): 12520.
63. Zarnetske, J.P., Haggerty, R., Wondzell, S.M., Bokil, V.A., González-Pinzón, R., 2012. Coupled transport and reaction kinetics control the nitrate source-sink function of hyporheic zones. Water Resour. Res., 48(11): W11508.
64. Zhang, L. et al., 2024a. Identification of surface water - groundwater nitrate governing factors in Jianghuai hilly area based on coupled SWAT-MODFLOW-RT3D modeling approach. Sci. Total Environ., 912: 168830.
65. Zhang, L., Wang, S., Wu, Z., 2014. Coupling effect of pH and dissolved oxygen in water column on nitrogen release at water–sediment interface of Erhai Lake, China. Estuarine Coastal Shelf Sci., 149: 178–186.

66. Zhang, S. et al., 2024b. Solute transport characteristics at the lakebed sediment-water interface due to multiple influences of dual seasonal lakes. Sci. Total Environ., 918: 170284.
67. Zhou, J. et al., 2021. Experimental and numerical investigations of the effect of imbricated gravel structures on flow and solute transport in a highly heterogeneous alluvial-proluvial fan aquifer, SW China. Environ. Fluid Mech., 21(1): 11–38.
68. Zhou, Y., Ritzi, R.W., Soltanian, M.R., Dominic, D.F., 2014. The Influence of Streambed Heterogeneity on Hyporheic Flow in Gravelly Rivers. Groundwater, 52(2): 206–216.
69. Zhu, Y., Dai, H., Yuan, S., 2023. The competition between heterotrophic denitrification and DNRA pathways in hyporheic zone and its impact on the fate of nitrate. J. Hydrol., 626: 130175.
70. Zhuang, T. et al., 2023. The influence of hyporheic exchange with spur dikes: Laboratory experiments. J. Hydrol., 622: 129754.
71. Zuo, R. et al., 2023. Groundwater table fluctuation: a driving force affecting nitrogen transformation in nitrate-contaminated groundwater. J. Hydrol.: 129606.

Figures

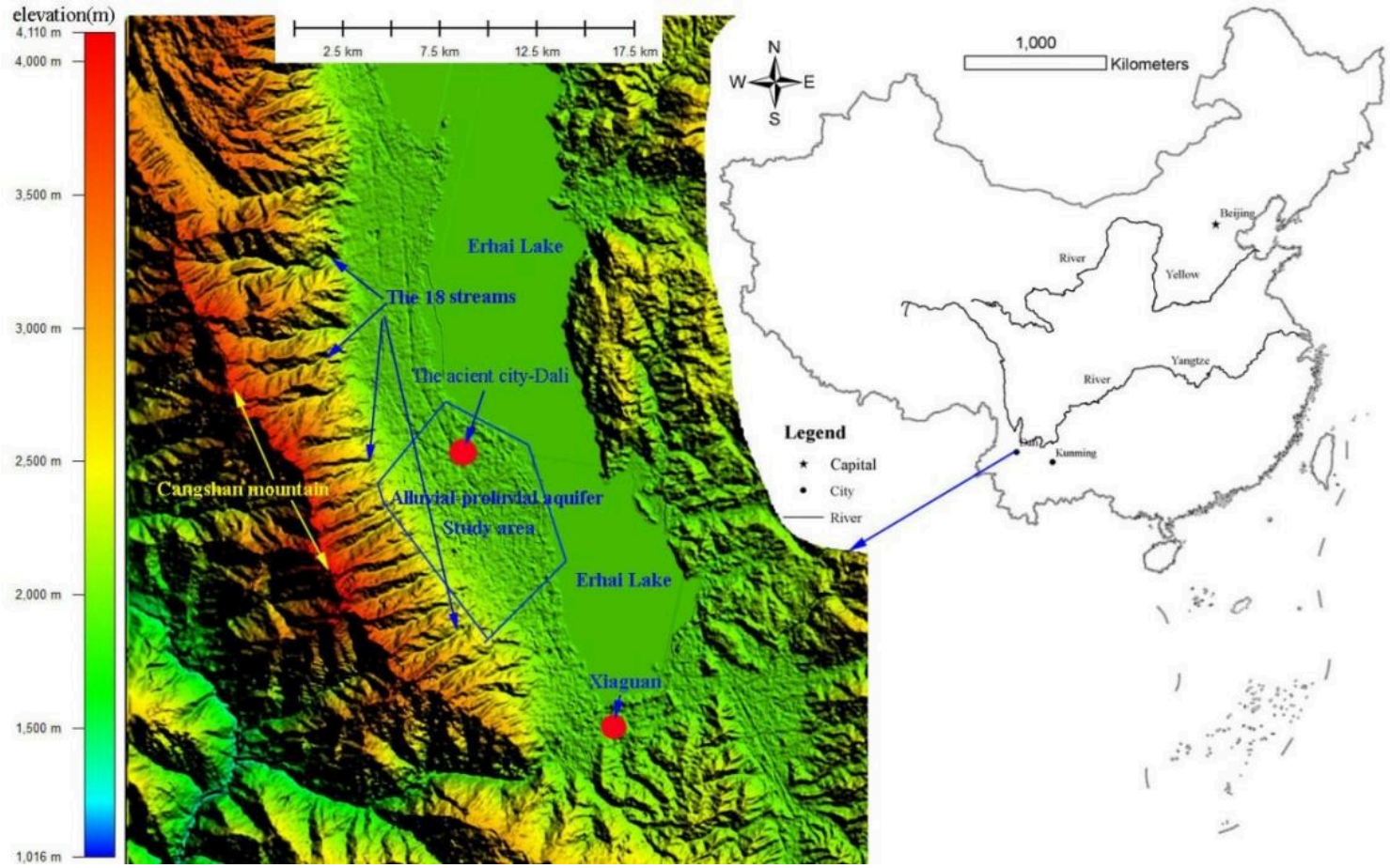


Figure 1

Location of the study area (Figure reference to Zhou et al. (2021))

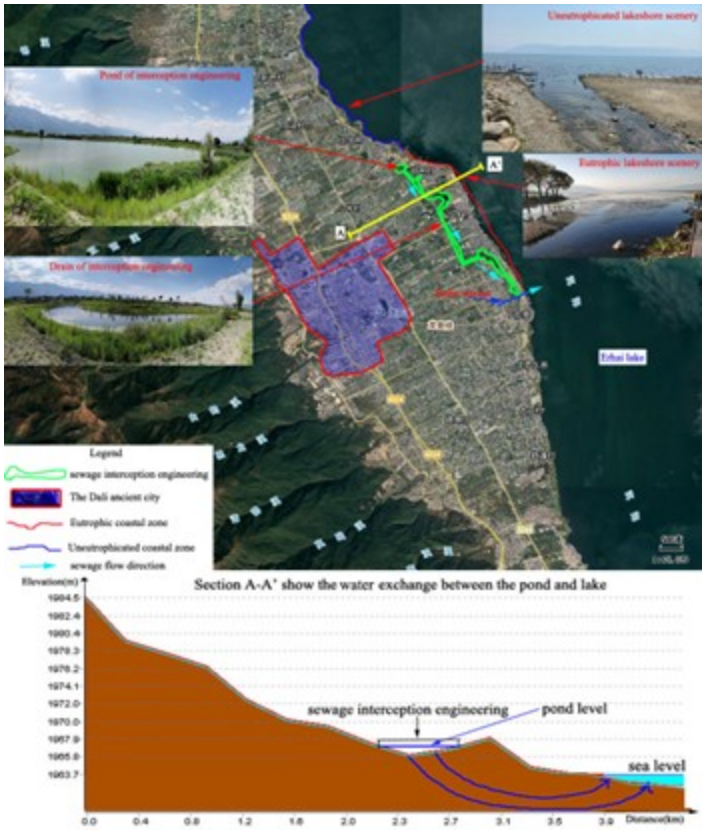


Figure 2

Map and figure showing the water exchange and nitrogen pollution in the study area



Figure 3

Map and figure showing the hydrogeology condition of the study area

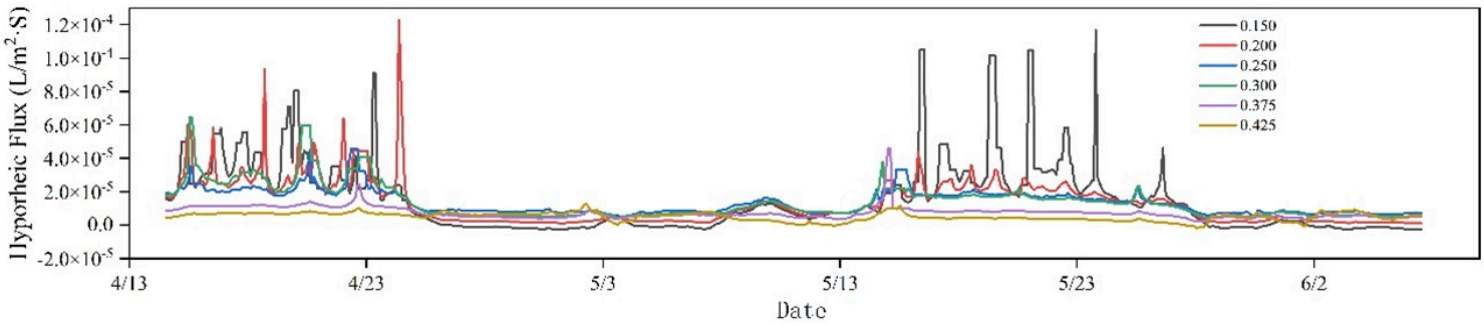


Figure 4

Hyporheic current flux diagram of Tao Stream from April 14 to June 6

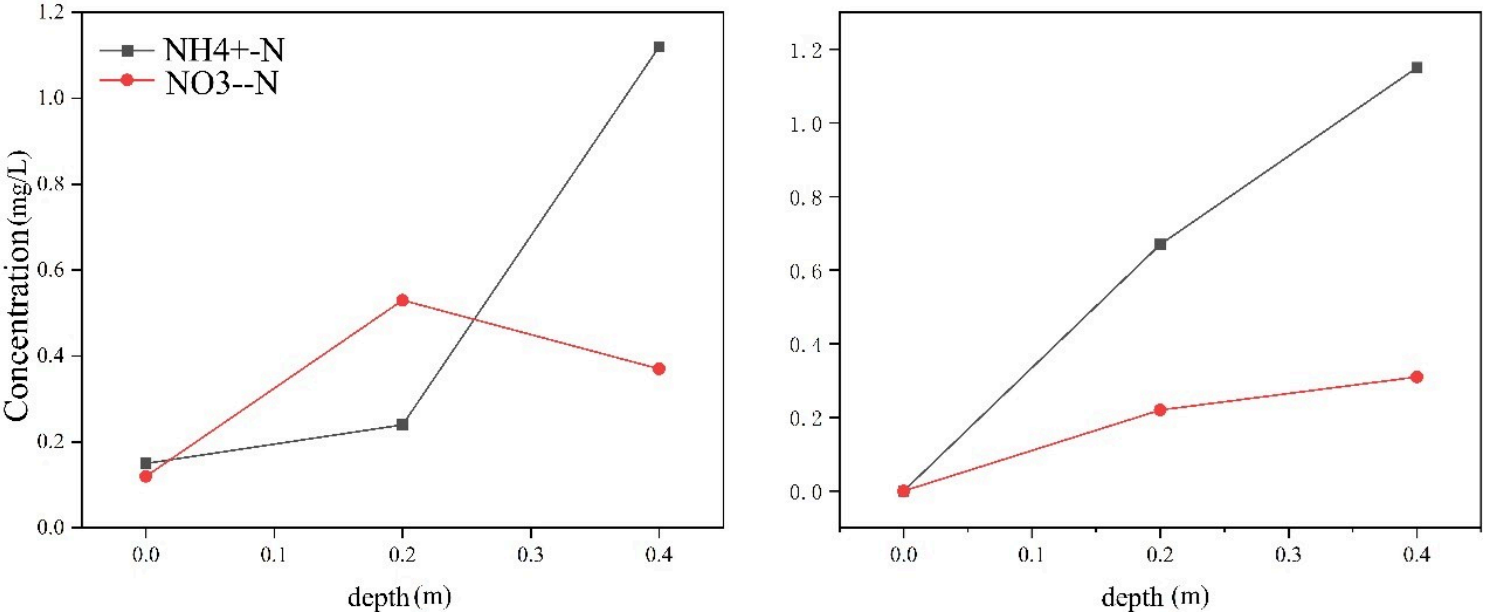


Figure 5

(a) Nitrogen content at different depths of bed sediments in the wet season

(b) Nitrogen content at different depths of bed sediments in the dry season

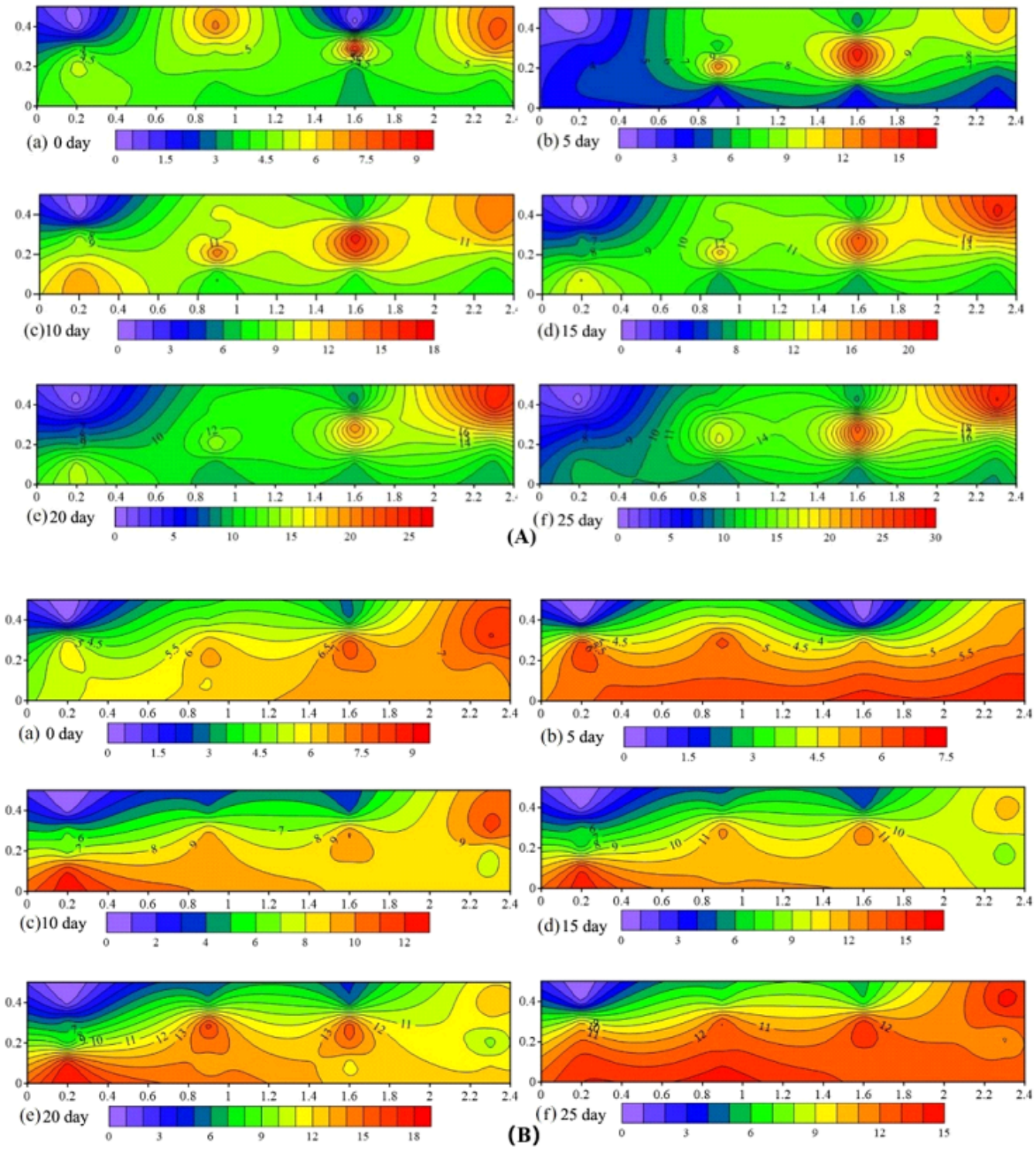


Figure 6

(A)Distribution of ammonia nitrogen concentration in Kriging interpolation box

(B)Distribution of nitrate nitrogen concentration in Kriging interpolation box

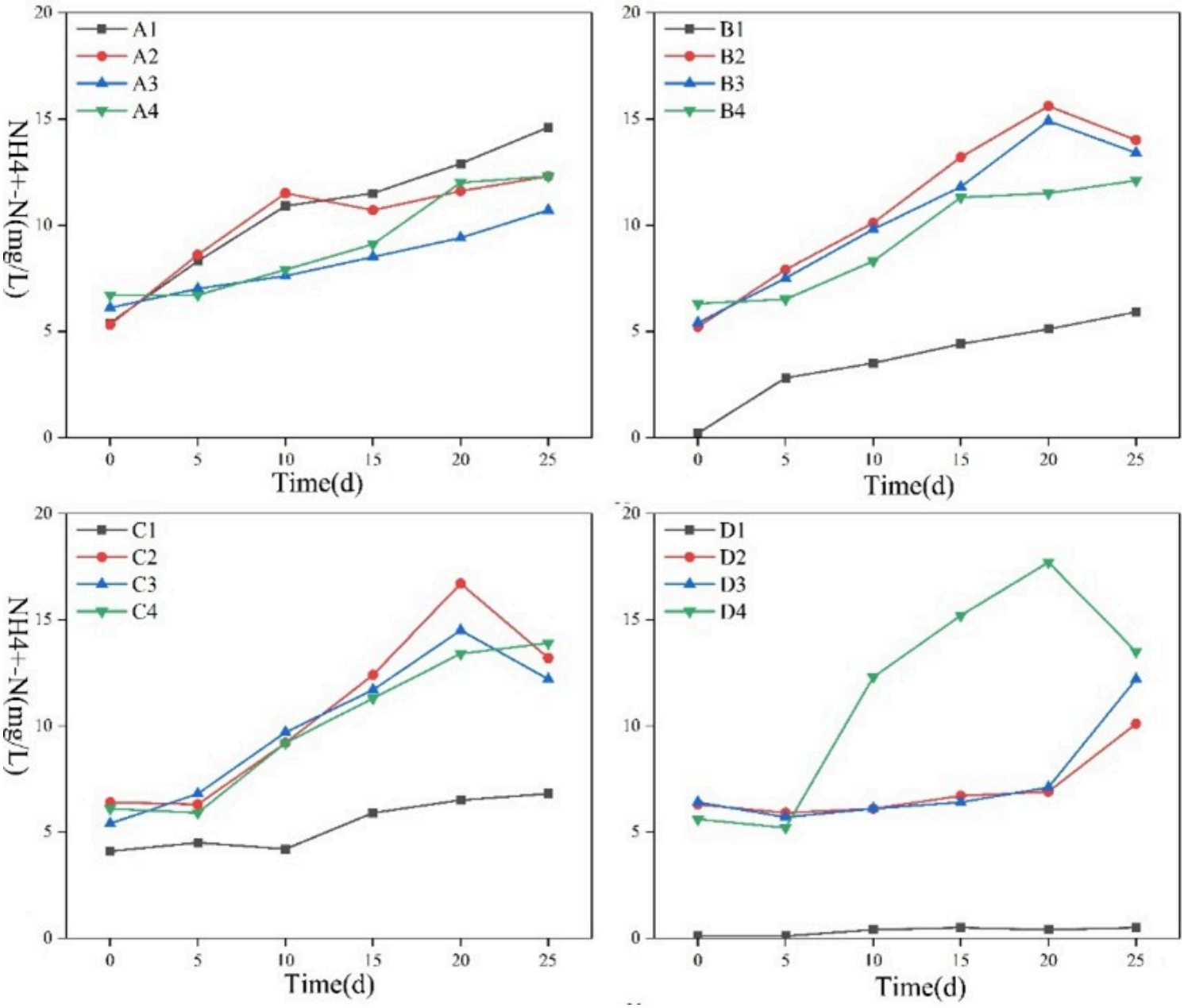


Figure 7

Variation of ammonia nitrogen concentration over time

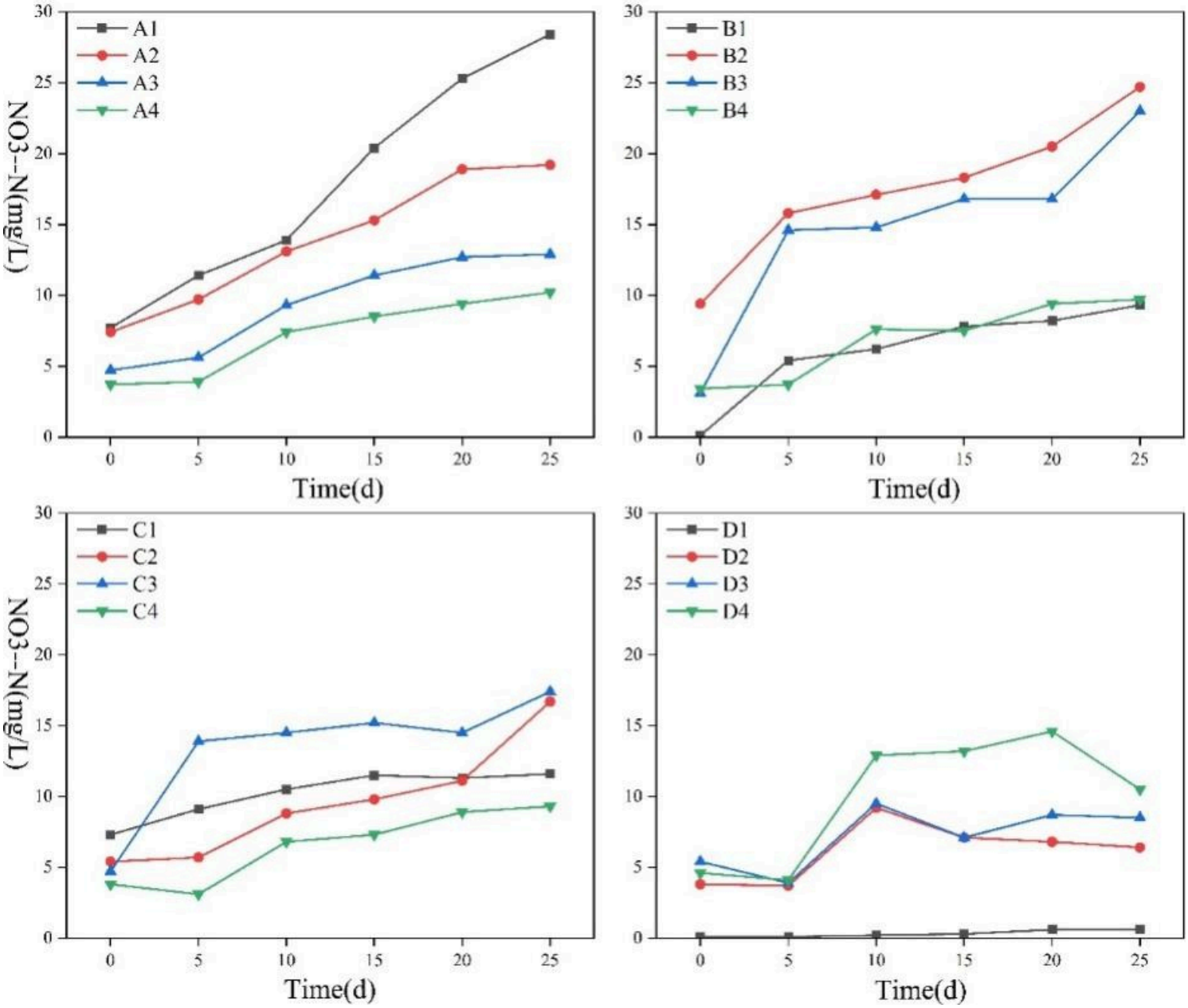


Figure 8

Variation of nitrate concentration over time

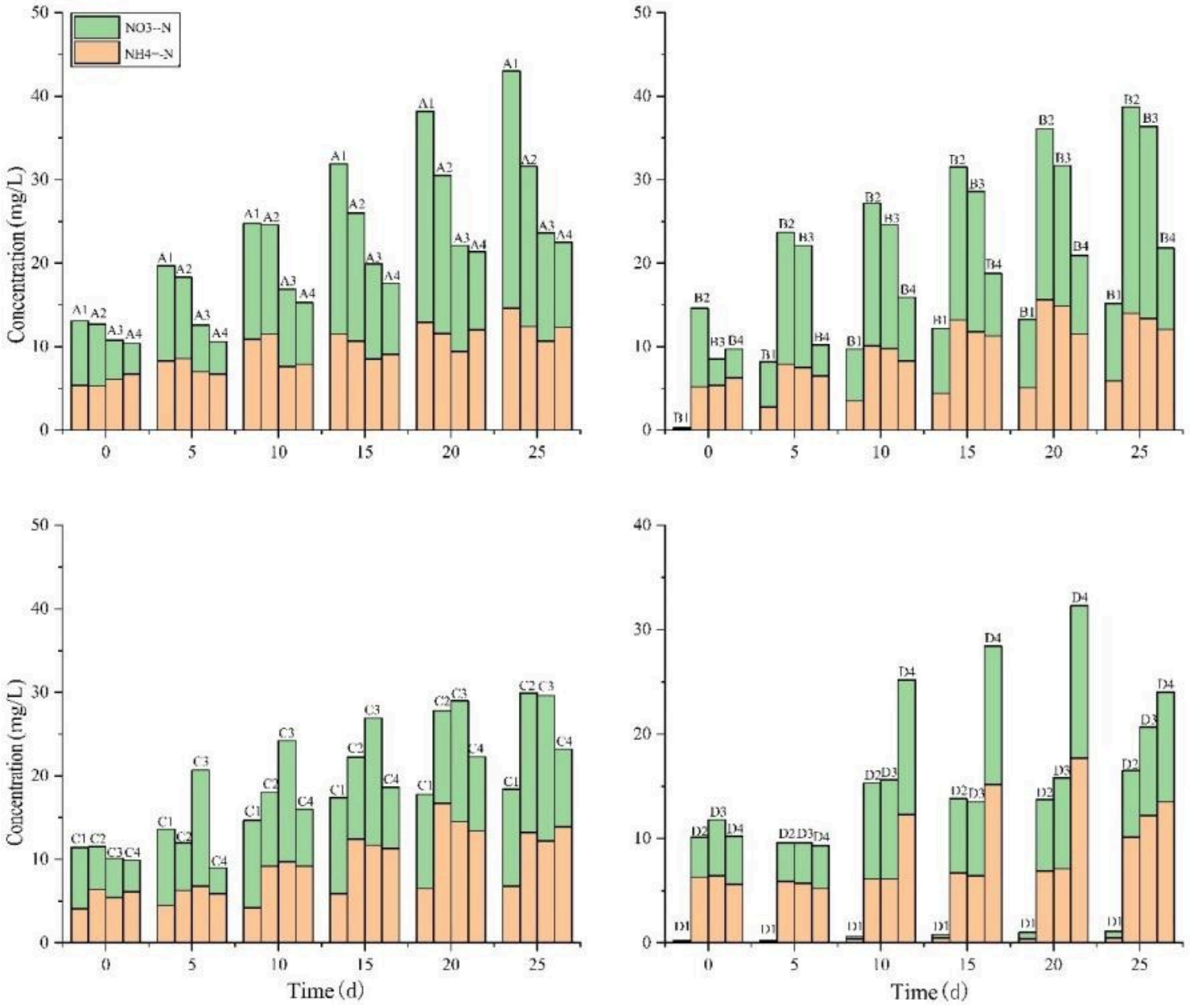


Figure 9

Accumulation diagram of ammonia nitrogen and nitrate nitrogen

Supplementary Files

This is a list of supplementary files associated with this preprint. Click to download.

- SupplementaryMaterial2025.10.28.docx